Finger Vein Recognition Using Pattern Matching and Corner Detection Strategies

K. Santhosh Kumar and D. Maheswari

Abstract---*Now-a-days, storing places are given with some kind of protection for security purpose like password, pin number or using any biometric identification system. For personal authentication, identification systems are used which utilizes Finger vein physiological biometric technology. This type of authentication is based on finger vein pattern's physical feature. In conventional techniques, combination of genetic algorithm and selection based on correlation filter are used to generate user-specific threshold in branch tracking step. Improved fuzzy clustering algorithm is used for deciding nearest points between samples. However in the vein extraction stage exact finding of the corner becomes very difficult task, to solve this issue, corner detection algorithm is utilized for features extraction (corner points) from the images of finger vein, where pattern matching is based on corner difference which is represented in point form using neural network classifier. Analysis is carried out on database of Hong Kong Polytechnic University (HKPU) to demonstrate the robustness of proposed technique with respect to accuracy, specificity, sensitivity, recall and Precision.*

Keywords--- *Biometric Identification, Personal Authentication, Physical Features and Neural Network.*

I. INTRODUCTION

In modern society, Biometric technology usage is getting significant increase. Voice recognition, iris recognition, fingerprint recognition, face recognition are the major research areas of biometric research. High attention is received by finger vein recognition in recent days. Medical research concludes that, various people's finger veins are different, on different fingers of same person, there is a variation in finger vein, in adults, finger vein pattern is not affected by time [1,2].

For biometric recognition, feasible and safe method is provided using finger vein. When compared with other characteristics of biometric like fingerprint, gait, face., there are two major advantages are available in finger vein. They are, identification of living body and internal characteristics. Living finger's vein only captured for processing and it is difficult to forge or copy it. Finger vein is highly robust to external damaging factors. So, in finger vein recognition is highly secured [3,4,5].

Because of these two major advantages, more attention is received from research teams by finger vein recognition. There exist, four major steps in conventional finger vein recognition process. They are, acquisition of finger vein image, pre-processing, extraction of features and recognition. There is a chance for false acceptance. In recent implementations, generated a user-specific threshold based on correlation filter, which is formed by combing genetic algorithm and selection process for enhancing template matching process's recognition performance [6,7, 8].

K. Santhosh Kumar, Research Scholar, Rathnavel Subramaniam College of Arts and Science. E-mail: bbksan@gmail.com
D. Maheswari , Research Coordinator, School of Computer Studies. PG, Rathinavel Subramaniam College of Arts and Science. E-mail: maheswari@rvsgroup.com

DOI: 10.37200/IJPR/V24I3/PR2020308
Received: 20 Feb 2020 | Revised: 28 Feb 2020 | Accepted: 14 Mar 2020

In branch tracking step, improved fuzzy clustering algorithm is used for deciding nearest points between samples. It is noticed that local vein branches nears to vein pattern's bifurcation point differ largely between fake images. And also in the vein extraction stage exact finding of the corner becomes very difficult task. To solve this issue in this work proposed work introduced one new method in which first corner detection algorithm is used for extracting finger vein image features and Branch tracking is done by using Improved Fuzzy Clustering. Based on corner difference, patterns matching is done which is represented points form using neural network classifier [9,10].

II. LITERATURE REVIEW

This section discusses about the review details of different recognition methods of finger vein using machine learning.

Yang et al[2014] investigated a soft biometric trait for enhancing finger vein recognition performance. In order to understand ancillary information, soft biometric trait's extraction conditions are proposed in first step. Phalangeal joint width which is extracted form images of finger vein directly are employed, is used based on these parameters .In order conduct finger vein pattern and width measurement, developed three frameworks. They are, hybrid, filter and fusion. On databases of open and self-built finger vein, experimentation is performed and exhibited a better performance, as shown by results of experimentation.

Yang et al [2018]proposed a unique finger impression and finger-vein based cancelable multi-biometric framework, which gives format assurance and revocability. The proposed multi-biometric framework joins the minutia-based unique finger impression highlight set and picture based finger-vein include set. Build up an element level combination methodology with three combination choices. Coordinating execution and security quality utilizing these distinctive combination alternatives are completely assessed and examined. Besides, contrasted and the first fractional discrete Fourier change (P-DFT), security of the proposed multi-biometric framework is fortified, because of the upgraded incomplete discrete Fourier change (EP-DFT) based non-invertible change.

Lu et al [2018] proposed another neighborhood descriptor, to be specific, pyramid histogram of twofold serious example (PHDCP). For a finger vein picture, the PHDCP first acquires a bank of sifted pictures utilizing Gabor channels with huge bit size and rich directions, by which the neighborhood line highlights are caught. At that point, the direction orders with the biggest and littlest reactions, which are the most powerful highlights, are chosen to produce an encoded map. At long last, a section segment based pyramid histogram extraction strategy is displayed to catch the various leveled highlights from the encoded picture. Numerical tests are led on two open finger vein informational indexes, MMCBNU_6000 and UTFVP. The test results exhibit that the proposed PHDCP performs far superior to the current nearby descriptors.

Huang et al [2016] presented a powerful and productive way to deal with dorsal hand vein acknowledgment. Rather than most of existing techniques, which either utilize surface highlights or shape highlights. A tale shape portrayal strategy is proposed to depict the geometry structure of the venous system, by incorporating both nearby and comprehensive investigations. Its similitude estimation is then progressively joined with that from the surface methodology, produced by the very much presumed surface administrator, in particular Local Binary Patterns

(LBP), for dynamic. The outcomes accomplished are better than the cutting edge ones so far revealed in the writing, which exhibits its viability.

Qin et al [2017] proposed another finger-vein extraction approach which identifies the valley-like structures utilizing the ebbs and flows in Radon space. Right off the bat, given a pixel, we acquire eight patches focused on it by turning a window along eight distinct directions and venture the subsequent patches into Radon space utilizing the Radon change. Furthermore, the vein patches make unmistakable valleys in Radon space. The vein designs are improved by the ebb and flow estimations of the valleys.

At long last, the vein organize is extricated from the upgrading picture by a binarization plot and coordinated for individual confirmation. The test results on both reached and contactless finger-vein databases show that our methodology can fundamentally improve the precision of the finger-vein confirmation framework

Yang et al [2018]proposed a cancelable finger-vein-based bio-cryptosystem, which not exclusively can give confirmation yet additionally can encode touchy social insurance information through a biometric cryptographic procedure, fluffy responsibility conspire (FCS). The proposed bio-cryptosystem stores both the encoded adaptation of medicinal services information and the biometric format on a brilliant card for the explanation that it is more secure if the biometric information never leaves the card. The work of the cancelable biometrics further upgrades the framework security. The exploratory outcomes and security examination show the legitimacy of the proposed conspire.

Kulkarni, et al [2016] used hidden biometric parameter termed as finger vein (FV) for proposing authentication system. Under finger skin, superficial vein pattern is captured using an implemented finger vein acquisition device. In human being, all fingers vein pattern are different and there is a difference in vein pattern of same person's fingers. Using normal eye, we cannot see this. The paper feature the essential set up of NIR based finger vein procurement gadget to catch the shallow vein design that shows the one of a kind highlights require for acknowledgment.

This Paper investigates the respective and differentiation constrained histogram balance procedure to improve finger vein crude examples caught by proposed finger vein obtaining. The presentation is checked utilizing Local Binary Pattern (LBP) calculation. The acknowledgment exactness is spoken to by chart between True Acceptance Rate (TAR) versus Genuine Rejection Rate (TRR). It is seen that TAR Vs TRR for standard information base is 94. 5% and for possess information base is 94.34%. It shows that FV has potential for individual ID.

III. PROPOSED METHODOLOGY

Working of finger vein recognition is explained elaborately in this section. There are seven stage in proposed system. They are, thinning and Denoising, corner detection, detection of bifurcation, tracking of branch, dot product and morphological dilation, user-specific threshold selection and identification. Proposed work's architecture is illustrated in figure 1.

DOI: 10.37200/IJPR/V24I3/PR2020308
Received: 20 Feb 2020 | Revised: 28 Feb 2020 | Accepted: 14 Mar 2020

International Journal of Psychosocial Rehabilitation, Vol. 24, Issue 03, 2020
ISSN: 1475-7192

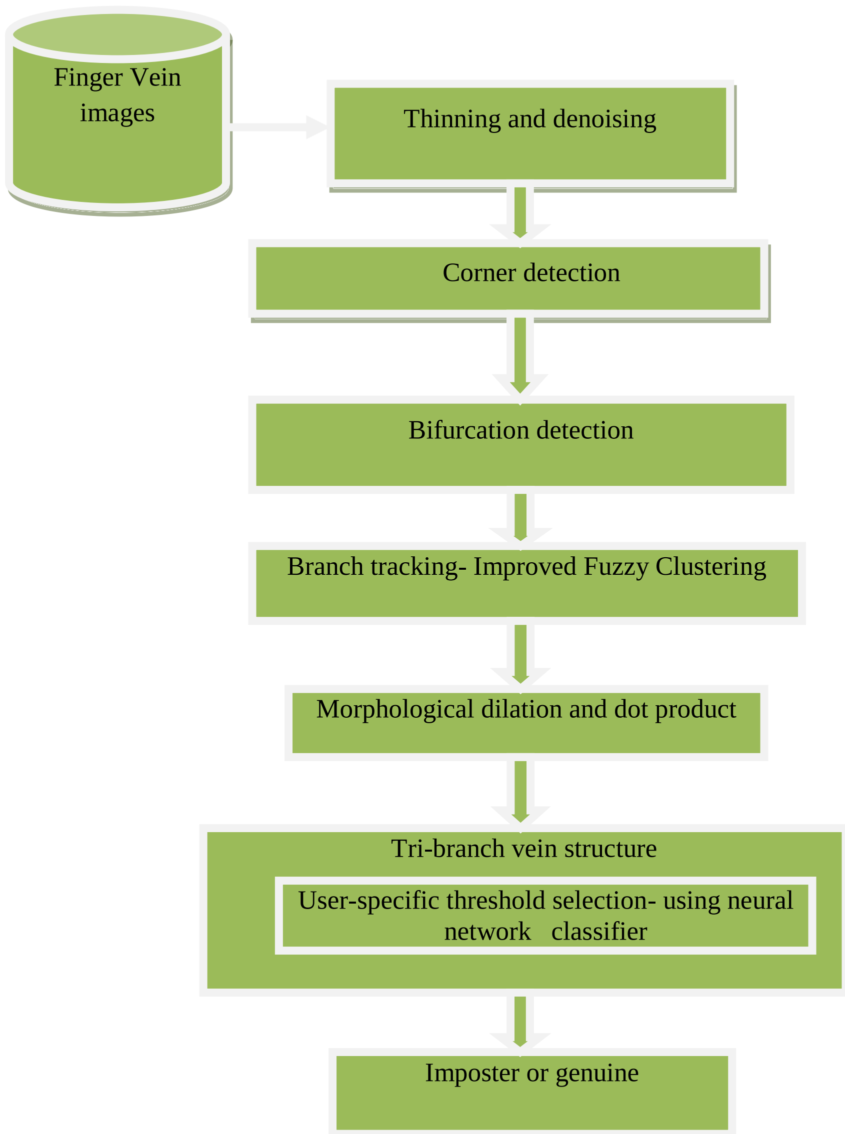

Figure 1: Overall Architecture of Proposed System

3.1. Thinning andDenoising

Skeletonization employed regions skeleton is obtained to perform thinning. Mathematical morphological operators are used in this work for computing this skeleton value. Miss or hit transform is related to this, in this work. Image I's thinning using structuring element J = (J_1, J_2) is expressed as,

$$Thin(i,j) = i - (i \otimes j) \quad (1)$$

Here, logical subtraction is performed and expressed as,

$$X\text{-}Y = X \cap Not\ Y \quad (2)$$

Until getting stabilised image, repeatedly applied this operation. This corresponds to convergence of an image. Structuring element sequence J is used in this work. Structuring element pairs (J_1^i , J_2^i) , i = 1..8 is used for thinning an image which produces image's connected skeleton. Morphological thinning operation is used for obtaining single-pixel wide vein network from vein pattern [18, 19].

DOI: 10.37200/IJPR/V24I3/PR2020308
Received: 20 Feb 2020 | Revised: 28 Feb 2020 | Accepted: 14 Mar 2020

Techniques used for acquisition and systems are introducing various kind of noises and artifacts in digital imaging field. Inferior visual quality of image and visibility of objects with less contrast are reduced due to this noise. So, there is a misclassification of bifurcation point as a intersection of vein branch and burr in vein network. Based on burr length, they are detected as well as removed due to the fact that,vein branch are higher in length when compared with burr [20].

3.2. Corner Detection using Harris Corner Detection Algorithm

There exist two classes of detection of comer in recent days. One class is based on detection of image gray comer and another is based on the algorithm of image edge extraction [21]. Algorithm of harris comer detection is a type of extraction operator, which is based on feature of signal point. Image's first derivative is only involved in this and its makes image window (j) which moves in all direction and its variation of intensity is expressed as,

$$E_{x,y} = \sum w_{x,v}\left[I_{x+v,y+v} - I_{w,v}\right]^2 (3)$$

$$=\sum_{w,v} xX + [yY + O(x^2, y^2)]^2 \ (4)$$

$$= Ax^2 + 2Cxy + By^2 (5)$$

$$= (x, y)M(x, y)^r (6)$$

Where, $M=\begin{bmatrix} A & c \\ c & B \end{bmatrix}$, in that, A=X2⊗ w, B=y2⊗ w, C = (XY) ⊗ w , first-order gray gradient is represented as X and Y, they are computed using image convolution,

$$X = \frac{\partial I}{\partial x} = I \otimes (-1,0,1) Y = \frac{\partial I}{\partial V} = I \otimes (-1,0,1) \qquad (7)$$

Image window is smoothened using Gaussian method for enhancing noise immunity and the following expression is used for settling Gaussian window,

$$w_{w,v} = \exp\left[-\frac{1}{2}(u^2 + v^2)/\delta^2\right] \qquad (8)$$

Two eigenvalues of M are set as λ_1 and $\lambda_2$and they are M's rotation invariants, they are proportional to local autocorrelation function's principal curvatures. Based on λ_1 and λ_1 values, edges, corners and flat areas are detected with following conditions,

(1) Flat area are represented by a small curvature of λ_1 and λ_1;

(2) Edge is represented by one small and one large value. It indicates the ridge-like shape of partial autocorrelation function. If there exist a high value of change in perpendicular direction of ridge, then change along ridge small.

(3) Corner are represented by large value of curvatures. This indicates a peak very intensive change across all direction. Comer Response Function (CRF) according to matrix M is expressed as ,

$$CRF = \det(M) - k.t^2(M) \quad (9)$$

Where, determinant of M is represented as det(M}, M's matrix trace is represented s t, constant is represented as k. Comer is point with local CRF maximum.

Flow of this work is described as,

DOI: 10.37200/IJPR/V24I3/PR2020308
Received: 20 Feb 2020 | Revised: 28 Feb 2020 | Accepted: 14 Mar 2020

Step I: Correlation matrix M is computed for everypixel (x,y) of gray image I;

Step 2: Corresponding pixel's comer score is estimated;

Step 3: Extracted comers count is limited by setting the threshold of CRF.[22,23].

3.3. Bifurcation Detection

In general, one bifurcation point is connected with three vein branches. In bifurcation's eight neighbour points between 0 to 1, switching number is six. Based on this developed a bifurcation detection method. Assume, p(x; y) as a current point and $\{P_i = p_1, p_2 \ldots p_8\}$ as eight neighbour points. If N_s of point p(x; y) is equal to 6, then it is said to be a bifurcation point and it is expressed as,

$$N_s = \sum_{i=1}^{8} |p_i + 1 - p_i|, \tag{10}$$

Where $p_9 = p_1$

3.4. Branch tracking using Improved Fuzzy c-means Clustering algorithm

In computer vision and image processing, because of its greater performance in clustering and simplified implementation, unsupervised clustering algorithm termed as Fuzzy c-mean clustering is most widely used.

FCM algorithm has following major drawbacks:

(1) To isolated point, sensitivity is exhibited by FCM algorithm.

(2) In FCM algorithm, clusters count c and fuzzy weighted index m needs to be predefined. Result of clustering is having direct impact of M and c.

(3) FCM algorithm may be stick with local optimum and it is not possible to find global optimum value.

Basic fuzzy c means algorithm is enhanced in this work for rectifying those issues.

3.4.1. An improved fuzzy C-means clustering algorithm

Presented an improved fuzzy C-means clustering algorithm in this work. Membership degree of data object is included with weight value and algorithm is incorporated with fuzzy clustering validity function in order to optimize clustering number c. This is the fundamental concept of this algorithm and is expressed as,

Initialization: Clustering number *c*is specified, $2 \leq c \leq n$, image pixel amount is represented as n, iterative threshold ε is computed with actual clustering pattern $P^{(0)}$and iterative counter $b = 0$.

***Step* 1**Partition matrix $U^{(b)}$ is updated or computed.

Step 2 Clustering pattern matrix $P^{(b+1)}$ for i □1…c is updated.

Step 3 Terminate the algorithm, if $p^{(b)} - p^{(b+1)} < \varepsilon$, and export the clustering pattern P and partition matrix U, else let b=b+1, go to Step 1.

Step 4 .Value of $FP^{(b+1)}$ (U; c) is computed, if $FP^{(b+1)}$ (U; c) <$FP^{(b)}$ (U; c) , then c = c +1, move to step 1, else, validity function FP (U; c) value is minimum, and clustering number c = c-1, terminate the clustering process.

Identified single-pixel wide tri branch vein structure using these steps.

DOI: 10.37200/IJPR/V24I3/PR2020308
Received: 20 Feb 2020 | Revised: 28 Feb 2020 | Accepted: 14 Mar 2020

3.5. Morphological Dilation and Dot Product

A new binary image is generated by performing morphological operationon binary image with a non-zero value of pixels for success test at particular position of input image. In this research work, on structure of single-pixel wide tri-branch vein, performed morphological dilation operation. Basic 8 ×8 matrix with 1 as an element value is used as structuring element. For matching purpose, tri-branch vein structures map is obtained using a dot product of entire vein pattern anddilated structure.

3.6. Correlation Filter Based User-specific Threshold Selection using Neural Network

In order to classify imposter and genuine images, neural network is used for computing finger vein images similarity form database.

Layer 1:

This layer is a fuzzification layer and each node *i* in this layer is a square node, which is expressed as,

$$O_i^1 = \mu_{A_i}(x)\ for\ i = 1,2 \quad (11)$$

$$O_i^1 = \mu_{B_{i-2}}(y)\ for\ i = 3,4 \quad (12)$$

Where, node *I*'s inputs are represented as *x* and *y* and input's fuzzy membership grade corresponds to output. Gaussian membership function is used in every node for computing input's degree of membership.

$$o_i^1 = \mu_{Ai}(x) = e^{\frac{-1}{2}\left(\frac{x-c_i}{\sigma_i}\right)} \quad (13)$$

Where, set of parameter is represented as$\{c,\sigma\}$, centre of membership function is represented as$C$ and width of membership function is represented as σ. These parameters are termed as premise parameters.

Layer 2:

Second layer is a rule layer, in which membership functions corresponds to input values and inputs are multiplied in every node to produce an output corresponds to a rule's firing strength. This layer output is expressed as,

$$O_i^2 = w_i = \mu_{A_i}(x)\mu_{B_i}(y),\ i = 1,2 \quad (14)$$

Layer 3:

Ratio of firing strength of *i*-th rule to sum of firing strength of rules defines *i*-th node of this layer.

$$O_i^3 = w_i = \frac{w_1}{w_1+w_2},\ i = 1,2 (15)$$

Layer 4:

Nodes in this layer are adaptive.

$$O_i^4 = w_i f_i = w_i(p_i x + q_i y + r_i) \quad (16)$$

DOI: 10.37200/IJPR/V24I3/PR2020308
Received: 20 Feb 2020 | Revised: 28 Feb 2020 | Accepted: 14 Mar 2020

Where, layer 3 output is represented as (w), set of parameters referring consequent parameter is represented as $\{p_i, q_i,\}$.

Layer 5:

This layer is having one fixed node and produces output as a sum of all incoming signal, which is represented as,

$$O_i^5 = \sum_{i=1} w_i f_i = \frac{\sum_i w_i f_i}{\sum_i w_i} \quad (17)$$

For each user, two input finger vein images similarity is computed based on layer function and stored this score of similarity. In order to avoid imposter images, enrolled users are matched with stored score of similarity.

3.6.1. Learning Model

In text summarization based on conventional fuzzy reasoning, ANFIS Learning Method's rules are decided by expert. In text summarization, this is a major limitation of fuzzy inference system (FIS). In ANFIS model, subtractive clustering method is used for generating rules automatically. There is no need of expert for deciding rules. Input-output training data are mapped to automatically compute centres of cluster and cluster number in subtractive clustering algorithm. Every instance is considered as a centre of cluster and first cluster corresponds to an instances with a value in first cluster range. Else, new cluster will be formed by these instances. Until including all instances into clusters, this process is repeated. Rules generated using clustering methods are highly tailored to data at the input when compared with rules generated without clustering. With high dimension input data, rules combinatorial explosion problem is reduced by this [24].

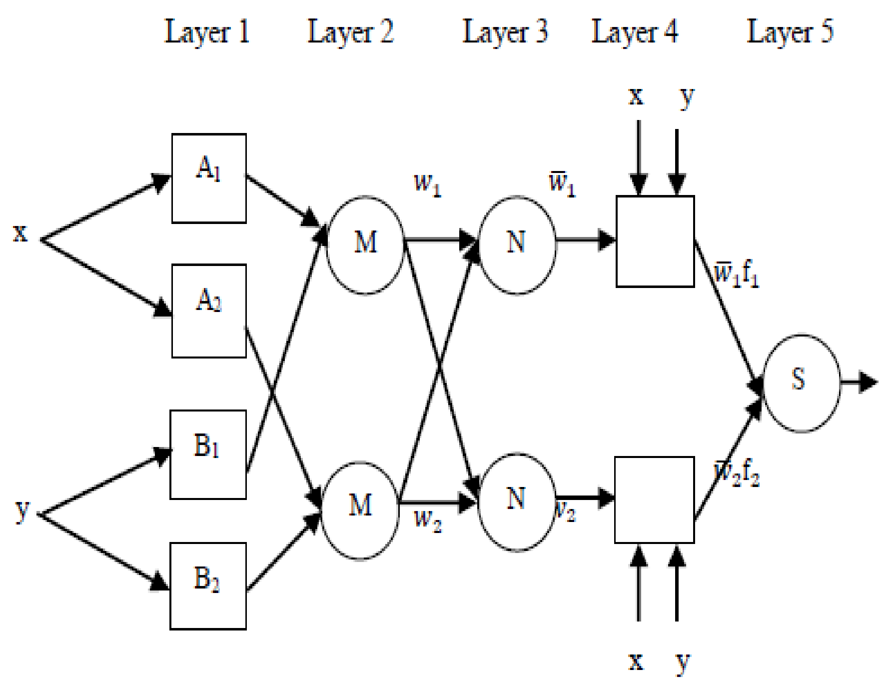

Figure 2: ANFIS Architecture

DOI: 10.37200/IJPR/V24I3/PR2020308
Received: 20 Feb 2020 | Revised: 28 Feb 2020 | Accepted: 14 Mar 2020

Hybrid method is formed by combining back propagation gradient descent technique and least-square estimation for training ANFIS model. Target output and actual output's squared error is minimized using Least-squares Estimate (LSE). Membership functions parameters are updated by combining LSE and back propagation method. From multilayer feed forward neural networks, origin of Back propagation is formed. Gradient descent method is used for computing network in order to minimizing sum of squared errors. Every input weight with learning rate, which will change as per time in every iteration is used in back propagation.

In hybrid optimization, included the backward and forward pass. Error measures are computed using forward pass. In backward pass, error rates are propagated to input end from output end, with the update of all parameters. Direct adjustment of membership functions parameters are enabled using the combination of membership functions having neural network's learning ability and fuzzy inference for representing knowledge in fuzzy rules form. After training, input data's membership function is illustrated in figure 4 [25].

3.6.2. Vein Classification

New input image's similarity is computed using a trained ANFIS model. For ANFIS, classification rules are set using the output of ANFIS model, which corresponds to similarity score. Experimental observation based similarity score is used for classifying predicted output to any on the classes. Root mean square error (RMSE) is produced in experimentation.

IV. RESULT AND DISCUSSION

This section introduces about the proposed methods results of experimentation. MATLAB2012 is used for implementing proposed method in the PC having 3.60GHzCPU and a memory of 12 GB.

Performance comparison is done between existing novel correlation filter based selection with genetic algorithm (CFBGN), user specific threshold based filtering (USCBF), Aanatomy Structure Analysis-based vein extraction (ASAVE) and proposed User Specific Threshold Selection Using ANFIS (USTS-ANFIS) with respect to false rejection rate, accuracy, recall and precision using finger vein images database called Hong Kong Polytechnic University (HKPU).

In this database, there exist 12 images for first 210 fingers which are captured in two sessions and there exist a 6 images for last 102 fingers which are captured in one session. Images are having 8-bit gray level and in BMP file format with 513_256 pixels resolution.

Table 1: Performance Comparison Results

Methods	**Precision**	**Recall**	**Accuracy**	**Error Rate**	**F-measure**
ASAVE	81.1900	83.4000	83.2500	16.7500	82.2950
USCBF	88.9181	88.9725	89.0244	10.9800	88.9453
CFBGN	91.8363	92.0033	91.8699	8.1300	92.0033
USTS-ANFIS	93.0866	93.0438	93.0894	6.9106	93.0652

DOI: 10.37200/IJPR/V24I3/PR2020308
Received: 20 Feb 2020 | Revised: 28 Feb 2020 | Accepted: 14 Mar 2020

International Journal of Psychosocial Rehabilitation, Vol. 24, Issue 03, 2020
ISSN: 1475-7192

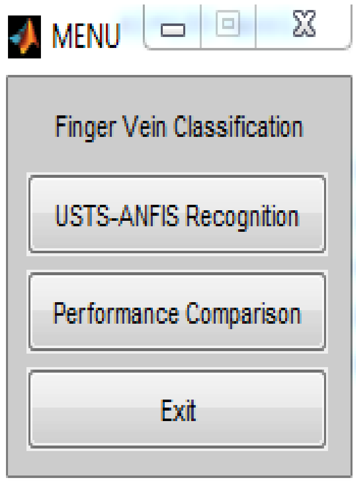

Figure 3:Menu

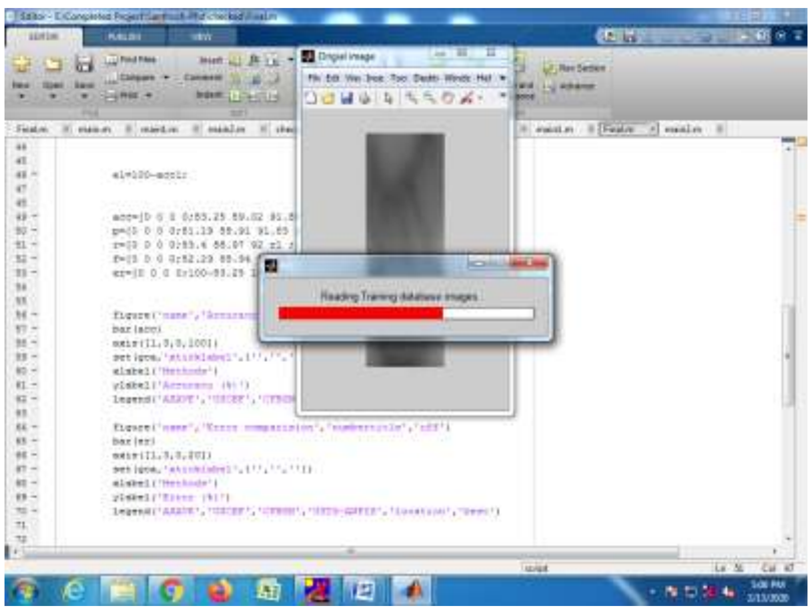

Figure 4: Reading Training Database Images

Segmented Image

Figure 5: Segmented Finger Vein Image

DOI: 10.37200/IJPR/V24I3/PR2020308
Received: 20 Feb 2020 | Revised: 28 Feb 2020 | Accepted: 14 Mar 2020

Extracted Vein Region and Thinning Image

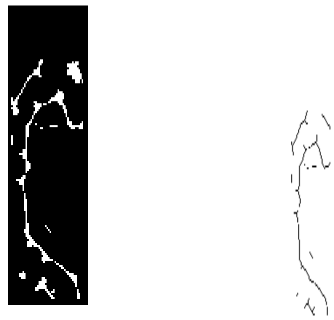

Figure 6: Extracted Vein Region and Thinned Region

Corner Detection

Figure 7: Corner Detected Image

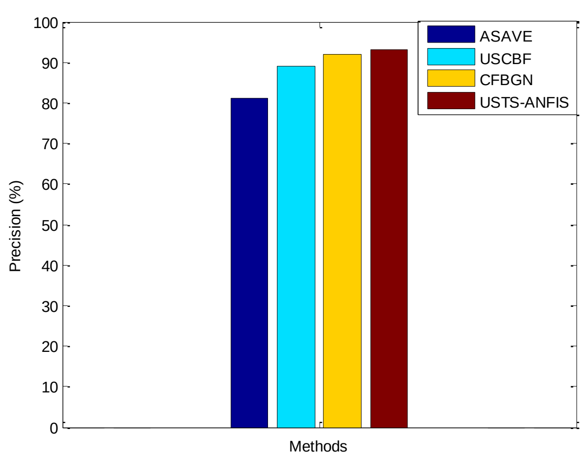

Figure 8: Precision Results of Different Method

DOI: 10.37200/IJPR/V24I3/PR2020308
Received: 20 Feb 2020 | Revised: 28 Feb 2020 | Accepted: 14 Mar 2020

Figure.8 illustrates Precision comparison of USTS-ANFIS, ASAVE, USCBF technique and novel CFBG. In X-axis, methods are represented and in Y-axis, value of precision is represented. It is concluded that proposed USTS-ANFIS has high precision value of 93.0866%, when compared with ASAVE technique which is having 81.1900%, USCBF with 88.9181% and novel CFBGN with 91.8363%.

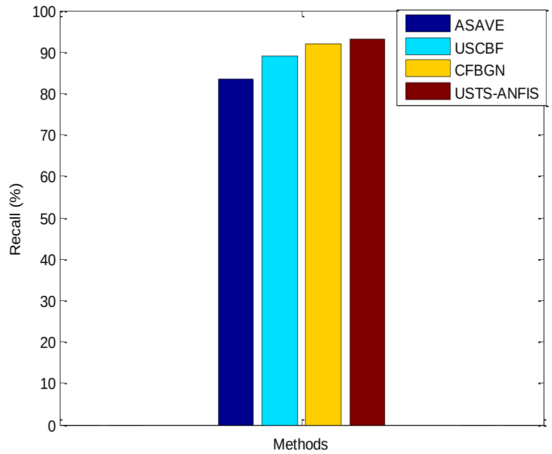

Figure 9: Recall Results of Different Method

Figure. 9 illustrates Recallcomparison of USTS-ANFIS, ASAVE, USCBF technique and novel CFBG. In X-axis, methods are represented and in Y-axis, value of sensitivity is represented. It is concluded that proposed USTS-ANFIS has high Recall value of 93.0438%, when compared with ASAVE technique which is having 83.4000%, USCBF with 88.9725% and novel CFBGN with 92.0033%.

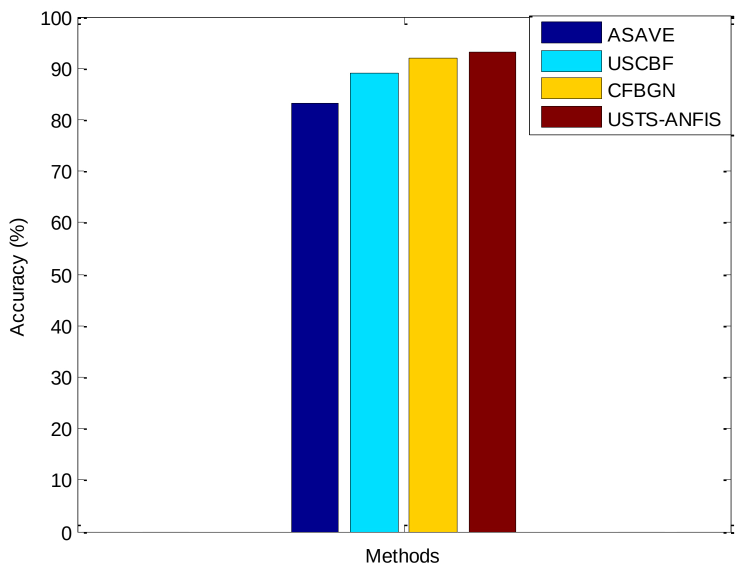

Figure 10: Accuracy Results of Different Method

Figure.10. illustrates Accuracy comparison of USTS-ANFIS, ASAVE, USCBF technique and novel CFBG. In X-axis, methods are represented and in Y-axis, value of accuracy is represented. It is concluded that proposed

DOI: 10.37200/IJPR/V24I3/PR2020308
Received: 20 Feb 2020 | Revised: 28 Feb 2020 | Accepted: 14 Mar 2020

USTS-ANFIS has high accuracy value of 93.0894%, when compared with ASAVE technique which is having 83.2500%, USCBF with 89.0244% and novel CFBGN with 91.8699%.

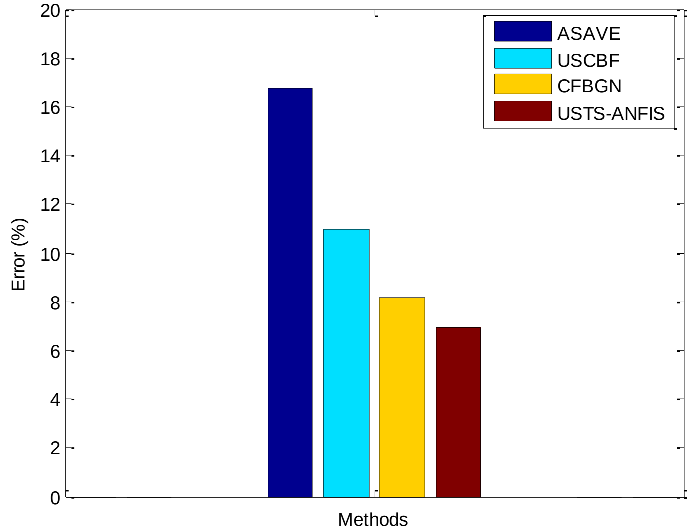

Figure 11: Error Rate Results of Different Method

Figure 11 illustrates Error rate comparison of USTS-ANFIS, ASAVE, USCBF technique and novel CFBG. It is concluded that proposed USTS-ANFIS has less error rate of 6.9106% , when compared with. ASAVE technique which is having 16.7500%, USCBF with 10.9800%, and novel CFBGN with 8.1300%.

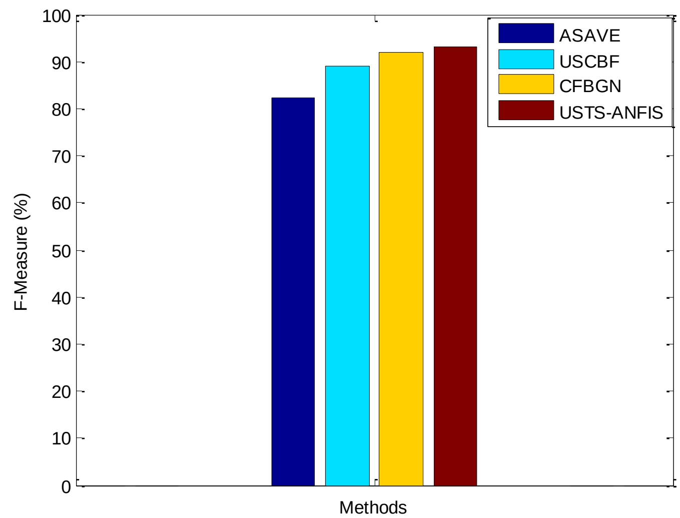

Figure 12: F-measure Results of Different Method

Figure 12 illustrates F-measure comparison of USTS-ANFIS, ASAVE, USCBF technique and novel CFBG. It is concluded that proposed USTS-ANFIS has around 93.0652% of F-measure value, while ASAVE technique has 82.2950%, USCBF has 88.9453% and novel CFBGN has 92.0033.

DOI: 10.37200/IJPR/V24I3/PR2020308
Received: 20 Feb 2020 | Revised: 28 Feb 2020 | Accepted: 14 Mar 2020

V. CONCLUSION AND FUTURE WORK

This work presented a finger vein recognition system with novel algorithm of finger vein recognition. In pre-processing phase thinning and Denoising is used to enhance the input finger vein image. Harris corner detection algorithm is used for detecting and extracting vein images corner in vein pattern extraction stage, Bifurcation points are tracked accurately to find Branch with the help of Improved Fuzzy c-means Clustering algorithm to find the vein pattern exactly, then Morphological dilation and dot product operations are used to map the extracted branch, finally adaptive fuzzy inference system is utilized to fine similarity score for classifying genuine and imposter image. Experimental results demonstrated that proposed model performs better with respect to Precision, Recall, accuracy. Due to low quality finger-vein input images, errors in segmentation may be produced during vein patterns extraction. So, in order to avoid these problems in future, some algorithms has to incorporated.

REFERENCES

[1] Sapkale, M. and Rajbhoj, S.M., 2016, August. A biometric authentication system based on finger vein recognition. In *2016 International Conference on Inventive Computation Technologies (ICICT)* (Vol. 3, pp. 1-4). IEEE.
[2] Wu, J.D. and Ye, S.H., 2009. Driver identification using finger-vein patterns with Radon transform and neural network. *Expert Systems with Applications*, *36*(3), pp.5793-5799.
[3] Sapkale, M. and Rajbhoj, S.M., 2016, August. A biometric authentication system based on finger vein recognition. In *2016 International Conference on Inventive Computation Technologies (ICICT)* (Vol. 3, pp. 1-4). IEEE.
[4] Sheeba, T. and Bernard, M.J., 2012. Survey on multimodal biometric authentication combining fingerprint and finger vein. *International Journal of Computer Applications*, *51*(5).
[5] Ibrahim, M.M.S., Al-Namiy, F.S., Beno, M. and Rajaji, L., 2011. Biometric authentication for secured transaction using finger vein technology.
[6] Sheeba, T. and Bernard, M.J., 2012. Survey on multimodal biometric authentication combining fingerprint and finger vein. *International Journal of Computer Applications*, *51*(5).
[7] Patil, P.A. and Ajmire, P.E., 2018. Survey: Human Identification Using Palm Vein Images. *Int J Emerging Technologies in Engineering Research*, *6*(3).
[8] Patil, P.A. and Ajmire, P.E., 2018. Survey: Human Identification Using Palm Vein Images. *Int J Emerging Technologies in Engineering Research*, *6*(3).
[9] Mulyono, D. and Jinn, H.S., 2008, April. A study of finger vein biometric for personal identification. In *2008 International Symposium on Biometrics and Security Technologies* (pp. 1-8). IEEE.
[10] Sree, S. and Radha, N., 2014. A survey on fusion techniques for multimodal biometric identification. *International Journal of Innovative Research in Computer and Communication Engineering*, *2*(12), pp.7493-7497.
[11] Yang, L., Yang, G., Yin, Y. and Xi, X., 2014. Exploring soft biometric trait with finger vein recognition. *Neurocomputing*, *135*, pp.218-228.
[12] Yang, W., Wang, S., Hu, J., Zheng, G. and Valli, C., 2018. A fingerprint and finger-vein based cancelable multi-biometric system. *Pattern Recognition*, *78*, pp.242-251.
[13] Lu, Y., Yoon, S., Wu, S. and Park, D.S., 2018. Pyramid histogram of double competitive pattern for finger vein recognition. *IEEE Access*, *6*, pp.56445-56456.
[14] Huang, D., Zhu, X., Wang, Y. and Zhang, D., 2016. Dorsal hand vein recognition via hierarchical combination of texture and shape clues. *Neurocomputing*, *214*, pp.815-828.
[15] Qin, H., He, X., Yao, X. and Li, H., 2017. Finger-vein verification based on the curvature in Radon space. *Expert Systems with Applications*, *82*, pp.151-161.
[16] Yang, W., Wang, S., Hu, J., Zheng, G., Chaudhry, J., Adi, E. and Valli, C., 2018. Securing mobile healthcare data: A smart card based cancelable Finger-Vein Bio-Cryptosystem. IEEE Access, 6, pp.36939-36947.
[17] Kulkarni, S., Raut, R.D. and Dakhole, P.K., 2016. A novel authentication system based on hidden biometric trait. Procedia Computer Science, 85, pp.255-262.

DOI: 10.37200/IJPR/V24I3/PR2020308
Received: 20 Feb 2020 | Revised: 28 Feb 2020 | Accepted: 14 Mar 2020

[18] Peng, Z. and Wang, G., 2017. Study on optimal selection of wavelet vanishing moments for ECG denoising. *Scientific reports*, *7*(1), p.4564.

[19] Anada, S., Nomura, Y., Hirayama, T. and Yamamoto, K., 2019. Electron Hologram Denoising via Sparse Coding and Dictionary Learning. *Microscopy and Microanalysis*, *25*(S2), pp.52-53.

[20] Marais, W.J., Holz, R.E., Hu, Y.H., Kuehn, R.E., Eloranta, E.E. and Willett, R.M., 2016. Approach to simultaneously denoise and invert backscatter and extinction from photon-limited atmospheric lidar observations. *Applied optics*, *55*(29), pp.8316-8334.

[21] Panchal, T., Patel, H. and Panchal, A., 2016. License plate detection using Harris corner and character segmentation by integrated approach from an image. *Procedia Computer Science*, *79*, pp.419-425.

[22] Ram, P. and Padmavathi, S., 2016, October. Analysis of Harris corner detection for color images. In *2016 International Conference on Signal Processing, Communication, Power and Embedded System (SCOPES)* (pp. 405-410). IEEE.

[23] Mistry, S. and Patel, A., 2016. Image Stitching using Harris Feature Detection. *International Research Journal of Engineering and Technology (IRJET)*, *3*(04), pp.2220-6.

[24] Jeyanthi, S., Maheswari, N.U. and Venkatesh, R., 2016. An efficient automatic overlapped fingerprint identification and recognition using ANFIS classifier. *International Journal of Fuzzy Systems*, *18*(3), pp.478-491.

[25] Jaya, B.K. and Kumar, S.S., 2018. Image Registration based Cervical Cancer Detection and Segmentation Using ANFIS Classifier. *Asian Pacific journal of cancer prevention: APJCP*, *19*(11), p.3203.

DOI: 10.37200/IJPR/V24I3/PR2020308
Received: 20 Feb 2020 | Revised: 28 Feb 2020 | Accepted: 14 Mar 2020